Astrophys Space Sci (2008) 315: 215–229
DOI 10.1007/s10509-008-9822-7

ORIGINAL ARTICLE

Enhanced luminosity of young stellar objects in cometary globules

G. Maheswar · H.C. Bhatt

Received: 3 February 2008 / Accepted: 21 April 2008 / Published online: 22 May 2008

Abstract In this study we investigated the effects of external trigger on the characteristics of young stellar objects (YSOs) associated with cometary globules (CGs). We made optical spectroscopy of stars associated with star-forming CGs. We find that the masses of the most massive stars associated with CGs are correlated with the masses of the parent cloud but they are systematically larger than expected for clouds of similar mass from the relation $M_{\text{max-star}} = 0.33 M_{\text{cl}}^{0.43}$ given by Larson (Mon. Not. R. Astron. Soc. 200:159, 1982). We have also estimated the luminosities of the IRAS sources found associated with CGs as a function of cloud mass and then compared them with those of the IRAS sources found associated with isolated opacity class 6 clouds (isolated and relatively away from large star forming regions). We find that the luminosities of IRAS sources associated with CGs are larger than those of the opacity class 6 clouds. These findings support results from recent simulations in which it was shown that the Radiation Driven Implosion (RDI) process, believed to be responsible for the cometary morphology and star formation, can increase the luminosity 1–2 orders of magnitudes higher than those of protostars formed without external triggering due to an increase in accretion rates. Thus implying that the massive stars can have profound influence on the star formation in clouds located in their vicinity.

Keywords ISM: clouds · ISM: globules · Stars: formation · Stars: pre-main sequence

G. Maheswar (✉)
International Center for Astrophysics, Korea Astronomy and Space Science Institute, 61-1 Hwaam-dong, Yuseong-gu, Daejeon 305-348, Republic of Korea
e-mail: maheswar@kasi.re.kr

G. Maheswar
Aryabhatta Research Institute of Observational Sciences, Nainital, 263129, India

H.C. Bhatt
Indian Institute of Astrophysics, Sarjapur Road, Koramangala, Bangalore, 560034, India

1 Introduction

Massive stars play a very vital role in star formation in giant molecular clouds. Strong radiation from massive stars impacts on the surrounding medium and may trigger further star formation. The effects of external radiation on a globule (or pre-existing clump) existing at the periphery of *HII* regions have been shown to lead to the Radiation Driven Implosion (RDI) of the globule (Bertoldi 1989; Bertoldi and McKee 1990). The cometary shapes of bright-rimmed clouds (BRCs) found at the periphery of relatively old *HII* regions were explained numerically by Lefloch and Lazareff (1994) applying RDI model without including self-gravity of the gas. Lefloch and Lazareff (1994) showed that the RDI process occurs in two phases; an early collapse phase during which the ionizing radiation compresses and ionizes the globule, probably forming Bright-Rimmed Clouds (BRCs), and a cometary phase in which the external ionized gas shields the tail from ionizing radiation and pressure confines the head, leading to a long-lived head-tail morphology as seen in Cometary Globules (CGs). The collapse phase is rapid, lasting about 10% of the lifetime of the globule. It is possibly in this phase that star formation occurs. Recently, SPH simulations have been performed by including self-gravity to investigate the effects of initial density

perturbations on the dynamics of ionizing clouds (Kessel-Deynet and Burkert 2003) and the evolution of the cloud morphology (Miao et al. 2006).

In BRCs, Sugitani et al. (1989, 1991) and Sugitani and Ogura (1994) have shown that the ratios of the derived luminosities of IRAS point sources associated with them and the mass of the parent clouds, i.e., $L_{\rm IR}$ to $M_{\rm cl}$ ratios, are higher (in the range $\sim$0.01–10^2 $L_\odot/M_\odot$) than those for the isolated dark globules (range between $\sim$0.03–0.3 $L_\odot/M_\odot$). They explained the difference of about two orders of magnitude by suggesting the formation of 3–4 times more massive stars in the BRCs. Similar results were obtained for clouds which are associated with *HII* regions (Dobashi et al. 1996). They found that the IRAS sources in the clouds associated with *HII* regions are systematically more luminous ($L_{\rm IR}/M_{\rm cl}$ was distributed from 1 to 10 $L_\odot/M_\odot$ for clouds with $M_{\rm cl} < 100$ $M_\odot$) than those associated with clouds away from *HII* regions (0.1 $L_\odot/M_\odot$ on average). Based on a study conducted on clouds from various locations of the Galaxy, which includes the BRCs studied by Sugitani et al. (1989, 1991) and Sugitani and Ogura (1994); Dobashi et al. (2001) have shown the presence of an upper and a lower limit to the luminosity distribution and suggested that the observed upper envelope might be limited by the star-formation efficiency (SFE). Motoyama et al. (2007), in their recent numerical simulations, found that the RDI mechanism can increase accretion rates of protostars near *HII* region by 1–2 orders of magnitude. This increase in the accretion rate results in luminosity 1–2 orders of magnitude higher than those of protostars formed without external triggering.

CGs are characterized by having compact, dusty heads (almost or completely opaque) with long, faintly luminous tails that extend several arc min in apparent length from one side of the head and a narrow, bright rim on the other side. Most of the CGs are found to be associated with star-forming regions with massive OB type stars (e.g., Hawarden and Brand 1976; Sandqvist 1976; Schneps et al. 1980; Zealey et al. 1983; Reipurth 1983; Gyulbudagyan 1986; Sugitani et al. 1991; Block et al. 1992; Ogura and Sugitani 1998). However, relatively isolated CGs are also known, for example CG 12 (Williams et al. 1977; Maheswar et al. 2004). The influence of some external source(s) on these objects is evident from their head-tail morphology. Studies suggest that the external trigger has influenced the internal properties of CGs. For e.g.:

- As a group, CGs are detected more frequently in ammonia than the other Bok globules (BGs) (75% compared with only 38%, Bourke et al. 1995 (B95)).
- The kinetic temperatures determined for some of the CGs ($T_K \sim$ 15–35 K, Harju et al. 1990; Cernicharo 1991; White 1993; Olano et al. 1994 (OWW94); González-Alfonso et al. 1995; B95) appears to be slightly higher when compared to darker globules ($T_K \sim$ 8–10 K, Dickman 1975; Myers and Benson 1983; Clemens et al. 1991; B95).

These results show that the same external forces which are responsible for the origin of these CGs may have modified their internal properties (like, density, temperature, etc.) also. There is evidence for current low mass star formation in a number CGs (Williams et al. 1977; Reipurth 1983; Brand et al. 1983; Pettersson 1984; Santos et al. 1998; Alcala et al. 2004). A number of CGs have IRAS point sources with SEDs characteristic of young stellar or protostellar objects, associated with their compact heads, indicating star formation at relatively enhanced rates (Bhatt 1993). Therefore if star formation in CGs are resulted due to external trigger, then the protostars and PMS stars found associated with them might be more luminous or massive when compared to those associated with clouds which are isolated and away from massive star forming regions.

In a study conducted by Larson (1982) to understand the initial mass function of stars, a correlation was found between the maximum stellar mass and the mass of the molecular cloud with which the star is associated. Similar correlation was obtained by Ho et al. (1981) between the maximum stellar masses and the mass of the molecular cloud cores. The mass of the most luminous stars and the mass of the parent clouds are related by (Larson 1982)

$$M_{\text{max-star}} = 0.33\ M_{\rm cl}^{0.43} \tag{1}$$

This result implies that the mass of the most massive star formed is related to the mass of the cloud with which it is associated. While the low-mass stars can form in clouds of all sizes, massive stars form only in massive clouds, together with large numbers of less massive stars. In this paper, we present results of a similar study carried out to investigate whether such a relation exist between the mass of the CGs and the mass of the most massive star currently associated with them. We also estimated the luminosities of the IRAS sources found associated with CGs as a function of cloud mass and then compared them with those IRAS sources which are found associated with the opacity class 6 clouds (isolated and relatively away from large star forming regions).

We begin with an updated list of CGs compiled from the literature given in Sect. 2. We present the details of the observations and data analysis in the same section. The Sect. 3 deals with the results and discussion concerning the correlation of the most massive optical source and most luminous IRAS source associated with the CGs to the parent cloud mass and their comparison with those of the isolated opacity class 6 clouds. We then summarize our conclusions in Sect. 4.

2 Observations and data analysis

2.1 The Cometary Globules list

We give an updated list of CGs compiled from the literature and from a search made by us in 100 μm IRAS images to identify clouds with cometary morphology in different locations of the Galaxy in Table 1. Column 1 contains the Right Ascension-ordered identification number of each globule, column 2 gives the globule identification, columns 3 and 4 give 2000.0 epoch Right Ascension and Declination. Columns 5 and 6 give the Galactic coordinates. Columns 7 and 8 contain remarks and references of individual globules respectively. Out of 92 CGs listed, twenty nine are associated with Orion OB 1 association, thirty two are associated with Gum nebula and rest are relatively isolated. The cloud identified with LBN 131.54-08.16, shown in Fig. 1, displays morphological features that are characteristic of CGs and we have therefore included it in our present study.

2.2 Optical spectroscopy

We obtained optical CCD spectra of sources with nebulosity (Ishii et al. 2002; Magakian 2003) and/or Hα emission (Herbig and Rao 1972; Herbig and Bell 1988; Ogura and Hasegawa 1983) found towards the direction of a number of CGs. Seven out of nine sources considered by us are known to be PMS stars (HBC 334, Thé et al. 1994; NSV 1832, Alcala et al. 2004; CPM 16, Campbell et al. 1989; HD 288313, Herbig and Rao 1972; Nx Pup, Thé et al. 1994; *h*4636, Williams et al. 1977; LkHα 233, Thé et al. 1994). As these young PMS stars should be near to their birth places and no other molecular clouds except corresponding CGs are present close to them, we believe that these stars are associated with the CGs. The spectra were obtained using the OptoMechanics Research (OMR) spectrograph (with a slit width of $\sim 2''$, wavelength range from 5800–7000 Å and resolution $\sim$1200) on the Vainu Bappu Telescope (VBT) at Kavalur and Hanle Faint Object Spectrograph Camera (HFOSC, with a slit width of $\sim 2''$, wavelength range from 5000–9000 Å and resolution $\sim$2000) on Himalayan Chandra Telescope (HCT) at Hanle during the period 2001–2005. The signal-to-noise ratio of the obtained spectra were $\gtrsim$30. All spectra were bias subtracted, flat-field corrected, extracted and wavelength calibrated in the standard manner using the IRAF.[1]

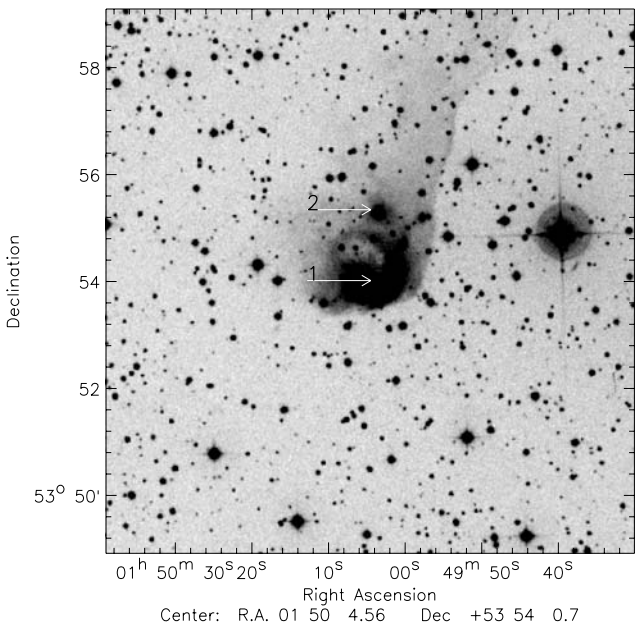

Fig. 1 We show a $10' \times 10'$ image of the field containing LBN 131.54-08.16. This image is reproduced from Digitized Sky Survey. We have marked the sources for which spectroscopic observations were carried out. North is *up* and east is to the *left*

2.3 IRAS measurements

The IRAS sources towards CGs and opacity class 6 clouds were taken from the catalog—IRAS catalog of Point Sources (IPAC 1989). We selected those IRAS sources which are located within the optical size and orientation of the cloud and have flux densities increasing with wavelength, a characteristic of young stellar or protostellar objects embedded in dark cloud.

3 Results and discussion

3.1 Maximum stellar masses of optical sources associated with CGs

Our spectroscopic results are presented in Table 2. In columns 1, 2 and 3 we give serial number, 2000.0 epoch Right Ascension and Declination respectively. In column 4 we indicate the presence and absence of Li (λ6707) and in columns 5 and 6 we give Hα (λ6563) equivalent widths ($W_{\mathrm{H}\alpha}$) and the spectral type of the sources respectively. The spectral types are determined by comparing the observed spectrum with those in the atlas of Jacoby et al. (1984). The spectral types determined here are uncertain by not more than two sub-classes. The spectrum of star 3, associated with LDN 1616 and identified with NSV 1832, shows Hα and O I (λ8445) line in clear emission. The presence of He I (λ6678) in absorption indicates that this star is an early type hot star. We have determined a B3 spectral type. Our spectral type determination is consistent with that estimated by Vieira et

[1]IRAF is distributed by National Optical Astronomy Observatories, USA.

Table 1 Literature data for program stars

S No.	Object Id.	$\alpha(J2000)$	$\delta(J2000)$	$l(°)$	$b(°)$	Remarks	Ref.
1	CB 06	00 49 29	+50 44.6	122.62	−12.13		1
2	IC 59	00 57 42	+61 05 00	123.69	−1.78		2
3	IC 63	00 59 01	+60 53 18	123.85	−1.97		2
4	LBN 131-08	01 50 05	+53 53 54	131.48	−8.21	Nebulosity	†
5	RNO 6	02 16 30	+55 22 57	134.88	−5.50	Nebulosity, Em* source	3
6	CB 26	05 00 09	+52 04 54	156.06	+6.00		1
7	[OS98] 01	05 04 24	−06 12 12	206.00	−26.59		4
8	[OS98] 02	05 06 20	−03 56 00	204.02	−25.11		4
9	[OS98] 03	05 06 48	−03 23 00	203.54	−24.75	HH objects, Nebulosity Em* sources	4
10	[OS98] 04	05 12 04	−01 55 36	202.83	−22.89		4
11	[OS98] 06	05 17 01	−07 44 36	209.09	−24.49		4
12	[OS98] 07	05 19 48	−05 52 05	207.60	−23.03	HH 240, Em* sources	4
13	[OS98] 10	05 20 50	−05 49 24	207.40	−22.94	Em* sources	4
14	[OS98] 12	05 22 11	−03 41 36	205.80	−21.50		4
15	Sim 130	05 22 55	+33 31 40	173.51	−01.58		5
16	Sim 129	05 23 09	+33 28 37	173.57	−01.57		5
17	[OS98] 16	05 26 54	−10 14 30	212.71	−23.38		4
18	[OS98] 17A	05 27 12	−10 28 42	212.98	−23.42		4
19	[OS98] 17B	05 27 01	−10 28 13	212.95	−23.45		4
20	[OS98] 25A	05 32 43	−02 55 42	206.39	−18.82		4
21	[OS98] 25B	05 32 29	−03 00 12	206.43	−18.91		4
22	[OS98] 29D	05 33 32	−01 36 18	205.25	−18.02		4
23	[OS98] 29K	05 34 40	−01 21.9	205.17	−17.66		4
24	[OS98] 29L	05 35 02	−01 15 48	205.12	−17.53		4
25	[OS98] 30	05 33 57	−03 41 42	207.26	−18.90		4
26	[OS98] 31	05 34 30	−02 58 15	206.65	−18.44		4
27	[OS98] 34	05 36 13	−04 00 42	207.83	−18.55		4
28	[OS98] 36	05 36 35	−04 01 12	207.88	−18.47		4
29	[OS98] 40A	05 38 05	−01 45 09	205.95	−17.09	HH 289	4
30	[OS98] 40B	05 37 54	−01 37 18	205.81	−17.07		4
31	[OS98] 40C	05 37 51	−01 35 36	205.77	−17.06		4
32	[OS98] 40D	05 37 52	−01 32 48	205.73	−17.04		4
33	[OS98] 41	05 38 26	−05 14 08	209.24	−18.61		4
34	[OS98] 42	05 38 51	−07 45 36	211.68	−19.65		4
35	[OS98] 45	05 39 42	−05 21 06	209.50	−18.38		4
36	[OS98] 46	05 40 18	−05 24 30	209.63	−18.28		4
37	[OS98] 47A	05 40 36	−05 25 00	209.67	−18.21		4
38	[OS98] 47B	05 40 58	−05 26 42	209.74	−18.14		4
39	[OS98] 55	05 41 08	−06 35 30	210.84	−18.62		4
40	[OS98] 56	05 41 37	−06 26 48	210.76	−18.45		4
41	[OS98] 59	05 43 07	−05 20 24	209.89	−17.62		4
42	[OS98] 60A	05 43 22	−05 01 00	209.62	−17.42		4
43	[OS98] 60B	05 43 52	−05 05 30	209.75	−17.34		4
44	[OS98] 61A	05 43 29	−03 35 30	208.31	−16.74		4
45	[OS98] 61B	05 43 32	−03 28 42	208.21	−16.68		4
46	[OS98] 62	05 47 24	+00 43 00	204.83	−13.87		4

Table 1 (*Continued*)

S No.	Object Id.	$\alpha(J2000)$	$\delta(J2000)$	$l(°)$	$b(°)$	Remarks	Ref.
47	LDN 1622	05 54 28	+01 48 12	204.70	−11.80	HH 122, Nebulosity, Em* sources	7
48	CG 1	07 19 22	−44 35 03	256.15	−14.07	Nebulosity, Em* source	6
49	CG 2	07 16 01	−43 57 42	255.31	−14.36		7
50	CG 3	07 39 13	−47 52 33	260.72	−12.40		7
51	CG 4	07 34 13	−46 54 24	259.44	−12.72		7
52	CG 5	07 40 52	−43 49 12	257.18	−10.27		7
53	CG 6	07 30 31	−46 43 48	259.00	−13.21		7
54	CG 7	09 14 19	−42 29 23	266.04	+04.31		7
55	CG 8	07 42 42	−41 15 44	255.06	−08.76		7
56	CG 9	07 40 48	−41 27 07	255.06	−09.17		7
57	CG 10	07 42 35	−42 05 23	255.79	−09.18		7
58	CG 13	07 14 11	−48 28 32	259.48	−16.43	Nebulosity	7
59	CG 14	07 38 38	−49 51 24	262.49	−13.37		7
60	CG 15	07 32 20	−50 45 48	262.88	−14.67		7
61	CG 16	07 27 36	−51 04 44	262.86	−15.48		7
62	CG 17	08 52 30	−51 52 00	270.58	−04.69		7
63	CG 18	08 52 30	−50 40 00	269.66	−03.91		7
64	CG 22	08 28 46	−33 44 14	253.58	+02.96	Em* source	7
65	CG 23	07 36 06	−50 13 00	262.64	−13.89		7
66	CG 24	08 19 16	−42 54 27	260.02	−03.82		7
67	CG 25	07 37 22	−47 57 05	260.65	−12.71		7
68	CG 26	08 16 00	−33 50 10	252.15	+00.73		7
69	CG 27	08 12 25	−33 45 16	251.66	+00.15		7
70	CG 28	08 12 22	−33 55 36	251.80	+00.05		7
71	CG 29	08 12 24	−34 00 58	251.88	+00.01		7
72	CG 30	08 09 33	−36 05 00	253.29	−01.61	HH 120	7
73	CG 31A	08 09 03	−36 01 18	253.19	−01.66		7
74	CG 31B	08 08 48	−36 03 00	253.18	−01.72		7
75	CG 31C	08 08 33	−35 59 00	253.11	−01.73		7
76	CG 31D	08 08 17	−36 01 48	253.11	−01.80		7
77	CG 31E	08 08 13	−36 04 06	253.13	−01.83		7
78	CG 32	08 14 24	−34 30 19	252.52	+00.08		7
79	CG 33	08 15 30	−34 04 34	252.29	+00.51		7
80	CG 34	07 29 36	−41 10 00	253.82	−10.90		7
81	CG 36	08 37 18	−36 37 56	256.95	+02.65		7
82	CG 37	08 12 28	−33 05 36	251.12	+00.53		7
83	CG 38	08 09 39	−36 10 36	253.38	−01.65		7
84	CG 21	12 37 09	−69 59 54	301.70	−7.16		8
85	CG 20	12 40 48	−69 51 00	302.01	−7.00		8
86	CG 19	12 45 42	−55 25 00	302.11	+7.45		8
87	CG 12	13 57 42	−39 56 21	316.49	+21.18	Nebulosity, Em* source	9
88	BHR 136	16 54 32	−40 31 06	344.52	+1.95		10
89	CG 11	19 40 30	−34 46 00	4.87	−24.54		9
90	CB 230	21 17 39	+68 17 32	105.17	+13.16	Nebulosity, sub-mm sources	1
91	Gal 096-15	22 34 30	+40 42 06	96.72	−15.10	Em* sources	11
92	Gal 110-13	23 37 39	+48 29 48	110.53	−12.59	Nebulosity	12

References: (1) Launhardt et al. (1997); (2) Jansen et al. (1994); (3) Bachiller et al. (2002); (4) Ogura and Sugitani (1998); (5) Marco and Negueruela (2003); (6) Magakian (2003); (7) Sridharan (1992); (8) Zealey et al. (1983); (9) Hawarden and Brand (1976); (10) Bourke et al. (1995); (11) Olano et al. (1994); (12) Odenwald et al. (1992)

Table 2 Results from spectroscopic observations of sources associated with CGs

S No.	$\alpha(J2000)$	$\delta(J2000)$	Li	$W_{H\alpha}$[a]	Sp.
LBN 131.54-08.16					
1	01 50 05	+53 54 01	–	3.7	B4
2	01 50 04	+53 55 18	–	5.3	A5
RNO 6					
1	02 16 31	+55 23 01	–	[b]	B1
LDN 1616					
1	05 06 51	−03 20 00	–	9.5	B9
2a	05 06 53	−03 20 54	yes	−2.1	K8
2b	05 06 53	−03 20 54	yes	−3.5	K3
3	05 06 56	−03 21 14	–	−59.0	B3
4	05 06 55	−03 20 05	yes	−55.9	K6
5	05 06 51	−03 19 38	yes	−4.3	M0
6	05 06 57	−03 18 36	yes	−1.9	M1
7	05 06 46	−03 19 23	yes	−1.7	M0
Sim 129					
1	05 23 08.3	+33 28 38	–	−70.3	B1
2	05 23 07.5	+33 28 38	–	[b]	B3
LDN 1622					
1	05 53 40.9	+01 38 13	yes	−43.6	K0
2	05 53 58.7	+01 44 09	yes	−34.1	K3
3a	05 54 03.0	+01 40 21	yes	–	K1
3b	05 54 01.9	+01 40 28	–	−17.6[c]	M3
4	05 54 08.0	+01 39 00	no	−46.9	M1
5	05 54 20.0	+01 42 56	yes	−34.4	K4
CG 1					
1	07 19 28	−44 35 10	–	−42.1	A2
Gal 96-15					
1	22 34 41	+40 40 05	–	−14.7	A7
2	22 34 25	+40 42 07	–	−253.7	K9
3	22 34 28	+40 42 04	yes	−32.2	K0
4	22 34 34	+40 42 16	yes	−46.5	K0
Gal 110-13					
1	23 37 52	+48 29 48	–	8.3	B8
2	23 37 18	+48 28 55	–	–	B9[d]

[a]Negative sign implies emission

[b]Emission within absorption

[c]$W_{H\alpha}$ from the slitless spectrum

[d]Spectral type from Aveni and Hunter (1969)

al. (2003) but not with Alcala et al. (2004). They have determined a K3 spectral type. The IRAS low resolution spectrum of NSV 1832 [from the catalog—IRAS Low Resolution Spectra] shows 9.7 µm silicate dust feature in absorption. Emission features corresponding to the stretching and bending vibrational modes at 9.7 µm arise when silicate dust is heated to temperatures of a few hundred Kelvin or more. This commonly occurs in the envelopes of luminous young stars embedded in their parent molecular clouds and in the extended atmospheres of cool, evolved stars with O-rich circumstellar shells. However, the circumstellar emission by warm dust and foreground absorption by cold dust may be superposed in the same line of sight towards an embedded star (Whittet 2003). The 9.7 µm feature seen in absorption in the spectrum of star 3 implies that this star is deeply embedded and the cold optically thick dust in its environment is absorbing the radiation. The visual extinction estimated towards this star, from $J-H$ color (2MASS) and assuming that the Rieke and Lebofsky (1985) reddening law can be applied to L1616 cloud, is ∼8 mag.

In Table 3, we present the properties of the most massive stars and the parent clouds. Columns 1 and 2 give the object identifications and the CGs with which the star is associated, respectively. Column 3 gives the spectral types of the most massive star associated with CGs. Though for majority of the sources Larson (1982) have estimated their masses by assuming them to be main sequence, for PMS sources their masses have been estimated from their position in the Hertzsprung-Russel (HR) diagram using the data of Cohen and Kuhi (1979). Since majority of the stars considered here are PMS, following the same procedure used by Larson (1982), we estimated masses of all the nine stars from their position in the HR diagram. To compute the luminosities of the stars and to locate them in the HR diagram, $V-B-V$ values were obtained from Simbad database except for CPM 16 and $h4636$. For CPM 16 and $h4636$, we obtained $V-B-V$ values from Maheswar et al. (2007) and Williams et al. (1977) respectively. The value of total-to-selective extinction (R_V) was taken to be 3.1. The color excesses ($E(B-V)$) were calculated from the observed $B-V$ colors and the intrinsic $B-V$ colors taken from Kenyon and Hartmann (1995) corresponding to the spectral type of the stars. The bolometric luminosity of the stars were computed using the equation $\mathrm{L_{bol}/L_{\odot}} = 10^{\frac{4.74-M_{\mathrm{bol}}}{2.5}}$, where 4.74 is the absolute bolometric magnitude of the Sun and M_{bol} is the absolute bolometric magnitudes of the stars computed from V, distance and extinction after correcting V using the values of bolometric corrections from Kenyon and Hartmann (1995). The masses of the stars were estimated using the evolutionary tracks of Palla and Stahler (1993). The value of R_V towards Herbig Ae/Be stars is found to be higher when compared to diffuse interstellar medium (Strom et al. 1972; Herbst et al. 1982; Gorti and Bhatt 1993; Hernádez et al. 2004). Therefore the choice of $R_V = 3.1$ would result in an under estimation of masses of the stars. For HD 288313 which is located above the birth line we quote lower limit on the mass. For stars HBC 334 and NSV 1832 which fall below the main sequence we adopt the masses corresponding to the ZAMS values for their spectral types. The estimated masses for the stars are given in column 4. The uncertainty in the estimated masses of stars are ∼1 $\mathrm{M_{\odot}}$. In

Table 3 Properties of the most massive star associated with CGs and those of the parent clouds

Object	Globule Id.	Sp. type	M_{max} ($M_\odot$)	M_{cl} ($M_\odot$)	Ref.
(1)	(2)	(3)	(4)	(5)	(6)
GSC 03684-01833	LBN 131.54-08.16	B4	5.8	200	[a]
HBC 334	RNO 6	B1	13.9	190	Ba
NSV 1832	LDN 1616	B3	7.6	180	Ra
CPM 16	Sim 129	B1	6.0	130	[a]
HD 288313	LDN 1622	K1	2.5	550	[b]
NX Pup	CG 1	A2	2.6	32[c]	Ha
h 4636	CG 12	B4	4.6	100	Wh, Ma
LkHa 233	Gal 96-15	A7	2.9	215	Ol
Sao 53209	Gal 110-13	B8	3.0	85	Od

[a]Mass estimated using (3) assuming $A_V = 5$ magnitude

[b]Mass estimated using (3) with estimated value of $A_V = 5.3$ magnitude (see Sect. 3.2.1)

[c]Mass of the entire cloud (32 $M_\odot$) is used instead of the mass of the globule head (4 $M_\odot$) in CG 1 as bulk (∼75%) of the mass is located in the tail

References: Ba—Bachiller et al. (2002); Ra—Ramesh (1995); Ha—Harju et al. (1990); Wh—White (1993); Ma—Maheswar et al. (2004); Ol—Olano et al. (1994); Od—Odenwald et al. (1992)

columns 5 and 6 we give masses of the CGs and references, respectively. For six clouds, the mass estimates from molecular line observations are available in the literature. The uncertainties in the CO isotope abundances and in the excitation temperature make the mass estimates to be uncertain by a factor of ∼2 which is in addition to the poorly known distance to these clouds (Vilas-Boas et al. 1994; Bachiller et al. 2002). The mass of LDN 1622 is estimated using (3) with an $A_V = 5.3$. In the case of two clouds, LBN 131.54-08.16 and Sim 129, we have used values of cloud masses estimated using (3) but with a common value of $A_V = 5$ (see discussed in Sect. 3.2). To find out the possible uncertainty in estimating masses using a common value of $A_V = 5$, we estimated the masses of those clouds for which mass estimation already exist in the literature. For example, CG 12 (our estimated value = 207 $M_\odot$, literature = 100 $M_\odot$; White 1993), CG 30 (8.3, 10; Nielsen et al. 1998), LDN 1616 (209, 180; Ramesh 1995), CG 1 (5.6, 4; Harju et al. 1990—*mass of the globule head alone*), CG 4 (5.6, 17; González-Alfonso et al. 1995), RNO 6 (400, 190; Bachiller et al. 2002) and Gal 110-13 (50, 85; Odenwald et al. 1992). The above results indicate that our mass estimates for LBN 131.54-08.16 and Sim 129 (using (3) with a common value of $A_V = 5$) may be uncertain by a factor of 2. In Fig. 2 we plot the mass of the most massive star associated with the CGs against the parent cloud mass. The dashed line represents the relation for the mass of the most luminous star and the mass of the parent cloud (see (1)) obtained by Larson (1982). It should be noted here that the Larson's relation given in (1) is based on samples from different locations and from different environments. In Fig. 2 we find that in 7 CGs, the mass of the most massive star formed is significantly

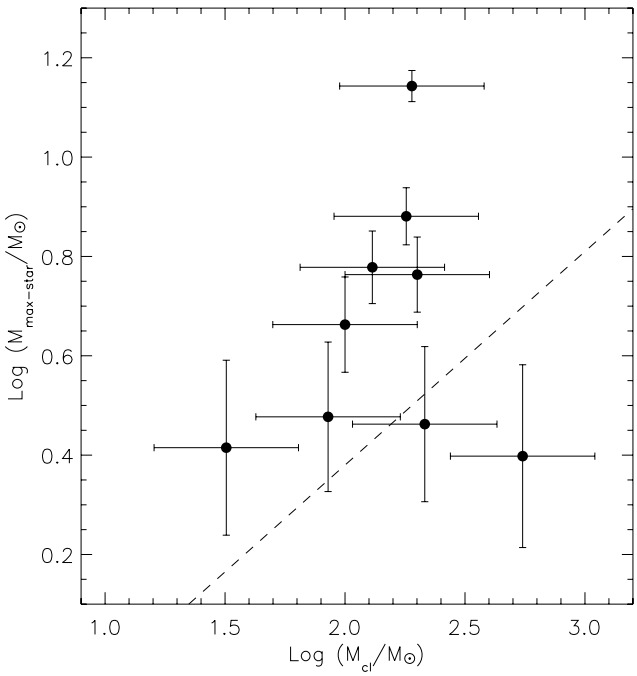

Fig. 2 The mass of the most massive star associated with CGs are plotted against parent cloud mass. The *dashed line* represents the relation for the mass of the most luminous star and the mass of the cloud (see (1)) given by Larson (1982)

higher than that represented by Larson's relation. This implies that stars formed in CGs are relatively more massive than those formed in isolated clouds of similar mass. If the star formation process in CGs produce young stars with a mass function similar to the Salpeter initial mass function, the increase in maximum stellar mass in CGs imply that the

total number of stars formed in these CGs are also higher. This will increase the SFE in these clouds.

In two CGs, LDN 1622 and Gal 96-15, the mass of the most massive star formed is found to be much lower when compared to other CGs. It may be that the star formation process in these clouds is not yet complete and the most massive star is yet to form. From the calibration of the Michigan class V stars in the range from A0 to G5 in terms of intrinsic Tycho-2 color $(B_T–V_T)_0$ and absolute magnitude M_{V_T}, Knude et al. (2002) have studied the extinction in the direction of LDN 1622. They suggested the existence of molecular material even at a distance as close as 160 pc. But whether LDN 1622 is at 160 pc is still unclear. It is however noteworthy that Bally (2001) in his discussion of the ISM structure in the Orion/Eridanus bubble remarks that the near side of this expanding bubble could be as close as 180 pc. The different radial velocities, $\sim$1 km s^{-1} and $\sim$10 km s^{-1} measured (Bally 2001) for L 1622 and L 1617 cloud (similar to Orion B cloud) respectively, might suggest that they belong to the near and far part of the expanding Orion bubble. If the distance of L 1622 becomes $\sim$160 pc, i.e., reduced by a factor of $\sim$3, then the mass of L 1622 (using (3)) will reduce by a factor of $\sim$9. But still the mass of the most massive star formed in L 1622 is found to be lower.

3.2 IRAS sources associated with CGs

In this section, the properties of the most massive IRAS sources positionally associated with the CGs and their parent cloud masses were compared with those of opacity class 6 clouds which are situated relatively away from large star forming regions. The masses of the clouds were estimated using the equation

$$M_{\rm cl} = \Omega D^2 \mu m_{\rm H} N_{\rm H} \tag{2}$$

where Ω and D are the angular area and distance to the globule respectively, μ is the mean molecular mass, $m_{\rm H}$ is the mass of a hydrogen atom and $N_{\rm H}$ is the number column density of hydrogen. Standard conversion formulae (e.g. Jenkins and Savage 1974) can be used to give the number column density from the extinction of the clouds as, $N_H = 2.5 \times 10^{21}\ A_V$. On expressing (3) in suitable units, the globule mass M in solar units is given as

$$M_{\rm cl} = 6.25 \times 10^{-3}.\Omega.A_V.D^2\ {\rm M}_\odot \tag{3}$$

where Ω is measured in square degrees, A_V in magnitudes and D in parsecs. The far-infrared luminosity of the IRAS sources were derived using the equation

$$L_{\rm IR} = 4\pi D^2 F_{\rm IR} \tag{4}$$

where $F_{\rm IR}$ is the total far-infrared flux estimated using Cox (2000)

$$F_{\rm IR} = (20.65S_{12} + 7.53S_{25} + 4.578S_{60} + 1.762S_{100}) \times 10^{-11}\ {\rm erg\,s^{-1}\,cm^{-2}} \tag{5}$$

We then derived the normalized IRAS luminosities per unit cloud mass, i.e., $L_{\rm IR}$ to $M_{\rm cl}$ ratios. In case of CGs with more than one IRAS source found, we have selected the one which is the most luminous.

The IRAS sources associated with 45 CGs are given in Table 4. Column 1 gives cloud identifications and column 2 gives IRAS source identifications [as given in the catalog "IRAS catalog of Point Sources, Version 2.0 (IPAC 1986)"]. The lifetime of the cometary stage in the RDI mechanism (Lefloch and Lazareff 1994) is found to be of the order of a few 10^5 yr to a few Myr. From the study of IRAS point sources found in Taurus-Auriga, Myers et al. (1987) showed that the stars in cores probably become visible T Tauri stars in less than 1×10^5 yr after they become detectable by IRAS, i.e., after they attain luminosity greater than $\sim$0.1 $L_\odot$. Therefore they are extremely young and may still be accreting and hence are primarily predecessors of T Tauri stars. The IRAS sources with SEDs characteristic of young stellar or protostellar objects (with their ages $\lesssim 10^5$ yr) associated with CGs, which are typically older (a few 10^5 yr to a few Myr), may have probably formed after the globules have experienced the external influence.

Column 3 gives the offset of IRAS sources from the cloud coordinates (coordinates quoted in the literature are in general correspond to the densest region of CGs). Columns 4, 5, 6 and 7 give IRAS flux densities (in Jansky) in 12, 25, 60 and 100 μm wavelength bands, respectively. We have selected those IRAS point sources which show an increase in flux towards the longer-wavelengths, a characteristic feature of YSOs. Column 8 gives the flux quality in each band. Columns 9 gives the distance of the globules from the Sun in parsec and the corresponding references in parenthesis. Distances of two CGs, LBN 131.54-08.16 & Sim 129, are estimated from the spectroscopic parallaxes of stars associated with them. Cometary globules appear to be composed of a dense head region and a less dense tail. Star formation is found to occur in the dense head part of the globules. We made a rough estimate of the radius of the head region of the globule by assuming a round shape with radius $R = w/2$ where w is the width of the head region. This procedure was adopted by Sugitani et al. (1991) to estimate the radii of type C (comet shaped) clouds. The optical angular area (in arc min^2) calculated using the estimated radius of the globules are given in column 10. The extinction A_V obtained from the literature are given in column 11 with the references in parenthesis.

In Table 5 we present the properties of IRAS sources found within the cloud boundaries of 29 Lynds opacity class

Table 4 Properties of IRAS sources associated with CGs

Object Id.	IRAS name	r (′)	S_{12} (Jy)	S_{25} (Jy)	S_{60} (Jy)	S_{100} (Jy)	Qly	D (Ref.) (pc)	Ω $(')^2$	A_V (Ref.)
(1)	(2)	(3)	(4)	(5)	(6)	(7)	(8)	(9)	(10)	(11)
CB 6	00465+5028	0.654	2.50e-01	1.01e+00	3.96e+00	8.96e+00	1333	800 (1)	9.13	–
IC 59	00547+6052	3.671	3.21e-01	6.09e-01	3.44e+00	6.62e+01	3312	230 (2)	12.64	–
IC 63	00560+6037	0.403	1.93e+00	2.52e+00	4.31e+01	7.43e+01	3333	230 (2)	3.16	–
LBN131	01467+5339	0.807	1.61e+00	1.94e+00	2.45e+01	7.17e+01	3333	2000[a]	5.80	–
CB 26	04559+5200	2.563	2.70e-01	3.19e-01	4.88e+00	1.11e+01	1133	300 (1)	16.00	1.8(11)
RNO6	02130+5509	0.154	2.57e+00	3.19e+00	3.32e+01	9.64e+01	3333	2000 (3)	12.64	–
Sim 129	05198+3325	0.064	8.32e+00	2.62e+01	1.46e+02	1.63e+02	3333	3400[a]	1.50	–
[*OS*98]01	05018-0616	1.558	2.72e-01	3.54e-01	5.79e-01	2.22e+00	1133	460 (4)	1.55	–
[*OS*98]02	05038-0400	0.553	2.50e-01	2.50e-01	8.18e-01	1.64e+01	1113	460 (4)	23.00	–
[*OS*98]03	05044-0325	1.078	1.31e+01	3.86e+01	2.32e+02	3.82e+02	3333	460 (4)	113.76	–
[*OS*98]04	05095-0159	0.480	2.50e-01	2.50e-01	1.55e+00	1.31e+01	1132	460 (4)	9.13	–
[*OS*98]06	05146-0747	0.126	2.50e-01	2.50e-01	1.97e+00	1.56e+01	1133	460 (4)	4.94	–
[*OS*98]07	05173-0555	0.010	2.50e-01	3.02e+00	2.71e+01	6.13e+01	1332	460 (4)	79.00	–
[*OS*98]10	05185-0552	0.591	2.50e-01	2.50e-01	1.59e+00	2.66e+01	1133	460 (4)	64.00	–
[*OS*98]16	05245-1017	0.824	2.50e-01	2.50e-01	6.62e-01	6.19e+00	1123	460 (4)	1.14	–
[*OS*98]25*B*	05299-0302	0.464	2.50e-01	2.61e-01	4.00e+00	3.39e+01	1231	460 (4)	6.64	–
[*OS*98]29*D*	05310-0138	0.701	3.26e-01	2.84e-01	3.93e+00	1.75e+01	1233	460 (4)	7.11	–
[*OS*98]29*L*	05324-0117	0.843	2.50e-01	2.63e-01	3.94e+00	1.28e+01	1123	460 (4)	3.16	–
[*OS*98]31	05320-0300	0.007	2.50e-01	3.50e-01	7.21e+00	2.50e+01	1323	460 (4)	10.82	–
[*OS*98]40*A*	05355-0146	0.004	3.84e-01	1.40e+00	1.33e+01	4.21e+01	3333	460 (4)	6.19	–
[*OS*98]41	05359-0515	0.012	1.44e+00	1.95e+00	1.89e+01	9.76e+01	3321	460 (4)	5.34	–
[*OS*98]45	05372-0522	0.283	4.13e-01	3.41e-01	7.89e+00	3.78e+01	1123	460 (4)	2.85	–
[*OS*98]59	05407-0522	1.565	2.95e-01	4.60e-01	7.95e+00	4.28e+01	1321	460 (4)	3.48	–
[*OS*98]60*B*	05414-0507	0.555	2.50e-01	3.33e-01	4.80e+00	3.54e+01	1312	460 (4)	1.34	–
LDN 1622	05513+0139	11.24	5.19e-01	1.16e+00	1.14e+01	4.52e+01	3321	450 (5)	316	5.3(11)
CG 1	07178-4429	0.772	6.68e+00	7.60e+00	1.31e+01	3.36e+01	3333	450 (6)	3.16	–
CG 2	07144-4352	0.370	2.50e-01	3.73e-01	4.41e-01	8.88e+00	1123	450 (6)	3.16	4.7(12)
CG 3	07378-4745	0.834	2.50e-01	2.50e-01	1.79e+00	1.31e+01	1133	450 (6)	3.55	–
CG 4	07329-4647	2.724	2.50e-01	3.79e-01	1.34e+00	5.82e+00	1331	450 (6)	3.16	5.6(13)
CG 5	07391-4342	1.616	2.50e-01	2.50e-01	9.37e-01	4.80e+00	1133	450 (6)	0.40	4.7(12)
CG 8	07408-4108	1.469	2.50e-01	2.50e-01	1.65e+00	8.44e+00	1133	450 (6)	0.79	–
CG 9	07389-4119	1.813	2.50e-01	2.50e-01	1.55e+00	5.97e+00	1133	450 (6)	0.80	–
CG 14	07372-4945	1.002	2.50e-01	2.50e-01	6.13e-01	8.92e+00	1123	450 (6)	2.37	5.0(12)
CG 22	08267-3336	1.086	3.95e-01	1.09e+00	3.20e+00	1.43e+01	3333	450 (6)	11.85	5.1(12)
CG 25	07358-4750	1.106	2.50e-01	2.50e-01	4.35e-01	3.88e+00	1113	450 (6)	0.20	–
CG 26	08140-3340	0.225	2.50e-01	2.50e-01	4.00e-01	3.31e+00	1113	450 (6)	2.00	6.0(12)
CG 27	08105-3335	0.926	2.50e-01	2.50e-01	4.00e-01	4.08e+00	1113	450 (6)	2.00	–
CG 28	08103-3346	0.833	2.50e-01	2.50e-01	6.43e-01	5.43e+00	1113	450 (6)	0.79	–
CG 30	08076-3556	0.008	6.30e-01	3.73e+00	1.82e+01	4.75e+01	3332	450 (6)	4.74	9.8(12)
CG 32	08124-3422	1.473	2.50e-01	2.96e-01	1.19e+01	4.05e+01	1333	450 (6)	3.56	7.6(12)
CG 19	12427-5508	0.759	2.50e-01	2.50e-01	2.23e+00	1.22e+01	1133	300 (7)	2.21	–
CG 12	13547-3944	2.382	7.81e+00	8.94e+00	6.75e+01	2.02e+02	3333	550 (8)	79.0	3.0(11)
BHR 136	16510-4026	0.647	9.62e-01	1.68e+00	1.59e+01	5.68e+01	3221	145 (9)	0.79	6.0(9)
CB 230	21169+6804	0.004	2.50e-01	6.83e-01	1.18e+01	3.35e+01	1333	450 (1)	17.70	1.4(11)
Gal 110-13	23353+4812	1.300	5.26e-01	7.13e-01	5.52e+00	3.71e+01	3331	440 (10)	30.0	2.9(11)

References: (1) Launhardt and Henning (1997); (2) Jansen et al. (1994); (3) Bachiller et al. (2002); (4) Ogura and Sugitani (1998); (5) Knude et al. (2002); (6) Sridharan (1992); (7) Bourke et al. (1995); Maheswar et al. (2004); (9) Vilas-Boas et al. (1994); (10) Odenwald et al. (1992); (11) This work; (12) Vilas-Boas et al. (1994); (13) González-Alfonso et al. (1995)

[a]Distance estimated from spectroscopic parallaxes of stars associated with the cloud

Table 5 Properties of IRAS sources associated with Lynds opacity class 6 clouds

Object	IRAS name	S_{12} (Jy)	S_{25} (Jy)	S_{60} (Jy)	S_{100} (Jy)	Qly	D (pc)	Ref.	Ω $(')^2$	A_V[a]	A_V[b]
(1)	(2)	(3)	(4)	(5)	(6)	(7)	(8)	(9)	(10)	(11)	(12)
LDN 43	16316-1540	1.50e+00	6.05e+00	3.53e+01	6.44e+01	3333	160	HL	84.97	2.1	2.5
LDN 111	17119-2027	2.50e-01	3.31e-01	4.00e-01	7.14e+00	1113	225	1	9.67	2.1	–
LDN 158	16445-1352	2.68e-01	3.34e-01	2.22e+00	3.26e+01	1132	160	HL	89.68	2.6	3.7
LDN 162	16459-1411	1.41e+00	1.90e+00	2.33e+00	6.47e+00	3313	160	HL	225.08	4.0	4.1
LDN 204	16444-1201	2.50e-01	3.53e-01	8.91e-01	1.18e+01	1133	170	HL	342.89	3.5	4.5
LDN 216	17347-1938	5.58e-01	4.76e-01	6.41e-01	6.49e+00	1113	160	2	29.01	1.5	–
LDN 219	17364-1946	2.55e-01	1.25e+00	1.02e+01	1.74e+01	1333	160	2	191.04	5.6	5.6
LDN 260	16442-0930	5.71e-01	3.31e+00	7.83e+00	7.54e+00	3333	160	HL	77.93	3.2	3.2
LDN 323	18126-1820	1.95e+00	4.15e+00	2.44e+01	3.78e+02	1311	200	HL	38.68	3.2	4.1
LDN 462	18046-0444	2.50e-01	3.84e-01	5.35e-01	6.32e+00	1113	200	CM	83.27	5.9	7.5
LDN 483	18148-0440	2.50e-01	6.91e+00	8.91e+01	1.66e+02	1333	200	HL	58.78	4.8	5.8
LDN 530	18474-0454	8.34e-01	1.17e+00	2.41e+00	5.82e+01	1131	350	HL	314.75	4.5	5.6
LDN 531	19037-0659	2.50e-01	4.98e-01	9.81e-01	9.84e+00	1332	400	HL	34.54	3.0	2.2
LDN 581	19051-0403	2.60e-01	3.40e-01	5.46e-01	6.15e+00	1113	200	CM	71.03	4.7	6.8
LDN 588	18331-0035	2.50e-01	6.06e-01	1.48e+01	3.49e+01	1333	200	CM	84.97	3.2	–
LDN 663	19345+0727	2.50e-01	2.50e-01	8.30e+00	4.20e+01	1133	250	HL	7.60	2.3	–
LDN 673	19184+1055	3.74e+00	5.46e+00	3.69e+00	9.69e+00	3312	300	HL	284.01	6.4	6.6
LDN 676	19187+1127	7.63e-01	8.66e-01	6.61e+00	9.67e+01	3311	300	3	15.20	4.8	–
LDN 677	19197+1126	5.85e-01	1.57e+00	5.70e+00	7.51e+01	1331	300	CM	9.67	3.2	–
LDN 769	19219+2300	2.50e-01	2.50e-01	2.77e+00	1.25e+01	1133	200	CM	142.71	3.3	3.7
LDN 1148	20395+6714	2.50e-01	2.50e-01	4.00e-01	2.82e+00	1113	350	HL	193.11	4.3	3.8
LDN 1246	23228+6320	2.62e-01	7.38e-01	2.06e+00	7.98e+00	2332	700	LH	9.67	1.4	–
LDN 1262	23238+7401	2.50e-01	7.76e-01	9.60e+00	1.52e+01	1333	200	HL	58.91	2.5	2.1
LDN 1535	04325+2402	2.50e-01	2.10e+00	1.29e+01	2.24e+01	1333	140	HL	108.99	3.0	3.9
LDN 1544	05013+2505	2.53e-01	3.87e-01	4.00e-01	3.33e+00	1113	140	HL	46.28	3.5	3.5
LDN 1551	04287+1801	1.00e+01	1.06e+02	3.73e+02	4.58e+02	3333	160	HL	110.21	4.6	3.3
LDN 1686	16235-2416	3.51e+01	2.65e+02	2.20e+03	4.64e+03	2333	160	HL	83.27	9.3	–
LDN 1709	16285-2356	3.07e-01	4.23e-01	1.01e+00	6.09e+01	1113	160	HL	268.47	4.0	5.0
LDN 1782	16394-1941	2.70e-01	5.09e-01	1.13e+00	1.28e+01	1132	160	CM	39.56	3.3	2.2

References: HL—Hilton and Lahulla (1995); LH—Launhardt and Henning (1997); CM—Lee and Myers (1999); 1—L111 is located close (∼30′) to L100 which is at a distance of 225 pc (Reipurth and Gee 1986); 2—The $V_{\rm lsr}$ velocity of L216 (10.4) & L219 (10.5) are similar to that of L226 (10.5) (Clemens and Barvainis 1988) which is located at distance of 160 pc (Launhardt and Henning 1997); 3—L676 is located close (∼30′) to L673 and L677

[a]This work

[b]Dobashi et al. (2005)

6 clouds obtained from Parker (1988). Of the 1802 optically selected dark clouds cataloged by Lynds (1962), 147 clouds are classified as class 6. Estimates of opacity of the Lynds clouds were made on a scale of 1 to 6, with the class 6 clouds being the most opaque with $A_V \gtrsim 5$ mag. These visual estimates were based on a comparison of the cloud with the neighboring fields for the particular Palomar photograph on which the cloud appeared. These clouds are generally

more compact than low opacity clouds and have more easily discernible boundaries. As we would find in later section (Sect. 3.2.1), that majority of the CGs have extinction $\gtrsim$5 mag, the comparison of the cloud properties and the properties of YSOs found associated with CGs with those of Lynds opacity class 6 clouds is reasonable. Parker (1988) has cataloged IRAS sources found lying within the boundaries of Lynds opacity class 6 clouds. Out of 147 opacity class 6 clouds, 73 clouds were found to contain IRAS sources which have $S_{100} > S_{25}$, where S_{100} and S_{25} are the 100 and 25 µm flux densities (Parker 1988). We have selected, from Parker's catalog, those IRAS sources which show an increase in flux densities with increasing wavelength. Column 1 of Table 5 gives cloud identifications, column 2 gives IRAS source identifications from the catalog, columns 3, 4, 5 and 6 give flux densities (in Jansky) in 12, 25, 60 and 100 µm respectively and column 7 gives flux quality in each band. Distance to the clouds and their references are given in columns 8 and 9 respectively. We have assigned a distance of 225 pc to L111 because it is located close (∼30′) to L100 which is known to be at a distance of 225 ± 25 pc from the Sun (Reipurth and Gee 1986). The $V_{\rm lsr}$ velocity of L216 (10.4 km s^{-1}) and L219 (10.5 km s^{-1}) are found to be similar to that of L226 (10.5 km s^{-1}) (Clemens and Barvainis 1988) which is located at distance of 160 pc (Launhardt and Henning 1997). Hence same distance is assumed for L216 and L219. Because of the close proximity (∼30′) of L676 to L673 and L677, which are estimated to be at a distance of 300 pc (Hilton and Lahulla 1995; Lee and Myers 1999) respectively, we have assigned 300 pc to L676 also. The optical angular areas of the clouds (in arc min^2) are given in column 10. The area of the clouds are estimated from the semi-major and semi-minor axes of the clouds given by Parker (1988).

3.2.1 *Estimation of visual extinction, A_V*

For calculating the cloud masses using (3), we required the values of A_V. We estimated the Av values using 2MASS data by following steps.

Step 1: 2MASS sources with photometric errors less than 0.1 magnitude in all the three bands were selected from (a) region within the cloud boundary (determined visually) (b) a nearby reference region (located within ∼1° from the cloud) which is relatively free from cloud material (determined visually).

Step 2: produced J–H, H–K color-color (CC) diagram for both the regions for each cloud (Fig. 3, shown as an illustration). We assumed that the Rieke and Lebofsky (1985) reddening law can be applied and also represents a reasonable approximation of the NIR extinction caused by the associated molecular material. Also plotted as solid lines in Fig. 3 are the locations of both unreddened main-sequence and giant stars (Koornneef 1983). From the extreme points of these curves we have plotted two dashed lines parallel to the Rieke and Lebofsky (1985) interstellar reddening vec-

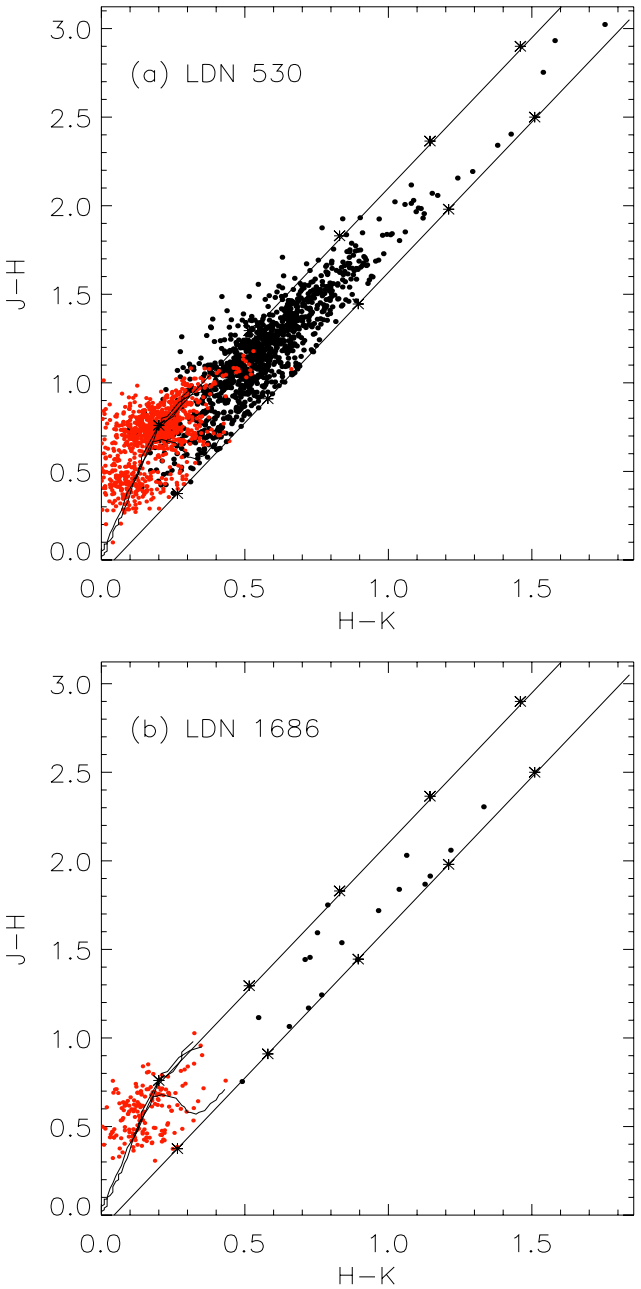

Fig. 3 (**a**) $J-H$, $H-K$ color-color (CC) diagram for LDN 530 given as an illustration to the procedure discussed in Sect. 3.2.1 as well as the best case where maximum number of 2MASS detections were available within the cloud boundary. *Solid lines* are the locations of both unreddened main-sequence and giant stars (Koornneef 1983). From the extreme points of these curves we have plotted *two dashed lines* parallel to the Rieke and Lebofsky (1985) interstellar reddening vector. Points marked with *asterisk* on the *dashed lines* are at an interval of $A_v = 5$ mag. (**b**) CC diagram for LDN 1686 shown as an illustration to the worst case where least number of stars were detected within the cloud boundary

tor. Points marked with asterisk on the dashed lines are at an interval of $A_v = 5$ mag. Any normal star affected by extinction will travel parallel to the reddening vector and will lie in the area between these lines corresponds to the reddening zone for normal stars. The region to the right of the reddening band is known as the infrared excess region (Lada and Adams 1992) and corresponds to the location of PMS sources. Sources falling in this region were rejected. However, naked-T Tauri stars, post-T Tauri stars and some class I sources do not show any near-IR excess, and will be found between the two reddening vectors in such a diagram [e.g., sources found in ρ Ophiuchus by Wilking and Lada (1983)]. But Ogura and Hasegawa (1983) suggested, from their Hα survey of the fields containing BGs, that there is a low possibility to find PMS sources near isolated BGs. Therefore we expect less contamination by PMS sources in the reddening zone.

Step 3: The value of $A_{\rm v}$ was estimated for each cloud using the relation, $A_{\rm v} = 9.4[(J–H) – (J–H)_o]$, where $(J–H)$ and $(J–H)_o$ are the mean value of colors for the cloud and corresponding reference regions, respectively. This procedure works well for those clouds which are closer to us (<300 pc) and, more importantly, whose angular sizes are sufficiently larger to have enough number of sources. In Figs. 3(a) and (b) we show the best (LDN 530, 1232 sources) and the worst (LDN 1686, 28 sources) cases, respectively.

Dobashi et al. (2005) have produced an atlas and catalog of dark clouds by applying traditional star-count technique to 1043 plates contained in the optical database "Digitized Sky Survey I". The catalog gives some of the physical parameters, such as the position, extent, and optical peak extinction of each clouds and clumps they have identified. Of the 29 opacity class 6 clouds studied here, 21 of them are identified in the catalog. Our A_V estimates (given in column 11 of Table 5) are in good agreement with the peak A_V values (given in column 12 of Table 5) given in the catalog. Because we used mean values of near-IR colors to estimate A_Vs, our values would represent extinction of clouds better than the peak values (estimated using optical star count) given in the catalog.

In the case of CGs we could use the above procedure to estimate A_Vs for only 5 of them. This is because, (1) majority of the CGs are of smaller angular sizes therefore not enough 2MASS detections to estimate A_Vs; (2) except two all others are at a distance >400 pc therefore there will be a significant number of unreddened or little reddened foreground sources which will make the mean $(J–H)$ color to move towards lower values resulting in an underestimation of A_V values; (3) a number of them show signs of current star formation due to which the reddening zone may get populated by PMS sources as well. Ogura and Hasegawa (1983) detected relatively more number of Hα sources near globules subjected to some external forces than near isolated ones. Our estimates of A_V values for 5 CGs, namely CB 26, LDN 1622, CG 12, CB 230, and Gal 110-13 are 1.8, 5.3, 3, 1.4, and 2.9, respectively. Of these for three of them, namely CB 26, LDN 1622, and CB 230, the peak values of A_V are given by Dobashi et al. (2005) as 1.4, 5.1, and 1.5, respectively. From $C^{18}O$ column density, Vilas-Boas et al. (1994) have estimated the values of A_V towards 17 CGs in Vela region using the relation, $A_V = 6.40 \times 10^{-15}\, N(C^{18}O) + 3.2$ magnitude. The peak A_V values for two CGs, CG 4 and CG 6, estimated by González-Alfonso et al. (1995) using ^{13}CO column density are found to be 5.6 and 5.1, respectively. Because CGs are compressed by the radiation from external source(s), they might be denser than the isolated BGs. This could be the reason why they are detected more frequently than the other BGs in ammonia (B95). The mean value of A_Vs estimated for CGs in Vela is found to be ∼5.5 magnitude. Therefore CGs for which A_V values are available (given in column 11 and respective references in parenthesis), we used them in (3) for the estimation of their masses. For the rest, we used a common value of $A_V = 5$ magnitudes for the mass estimation.

3.2.2 *The $L_{\rm max}$-$M_{\rm CL}$ relation*

The luminosities of IRAS sources found towards CGs and opacity class 6 clouds are plotted against their parent cloud mass in Fig. 4(a). Open and filled circles represent CGs and opacity class 6 clouds respectively. The luminosities of IRAS sources found towards CGs are in the range ∼0.3–4×10^3 $L_\odot$ and that of opacity class 6 clouds are in the range ∼0.03–2×10^2 $L_\odot$. In Fig. 4(a), we find that the maximum luminosity of the IRAS sources increases along with the parent cloud mass in the cloud mass range ∼1–10^3 $M_\odot$. This shows that the parent cloud mass is a decisive parameter influencing the population of massive stars. Besides, the maximum luminosity of the IRAS sources found associated with CGs are systematically more luminous (roughly by one order of magnitude) than those found towards the opacity class 6 clouds for a range of parent cloud masses (∼1–500 $M_\odot$). This indicates that brighter and more massive stars could form in clouds which are influenced by external forces.

In order to eliminate the uncertainties in the determination of $L_{\rm IR}$ and $M_{\rm cl}$ due to uncertainties in the distance estimation, we calculated normalized IRAS luminosity per unit cloud mass, $L_{\rm IR}/M_{\rm cl}$, for both CGs and opacity class 6 clouds. Both $L_{\rm IR}$ and $M_{\rm cl}$ being proportional to $(distance^2)$, the ratio $L_{\rm IR}/M_{\rm cl}$ is independent of distance. In Fig. 4(b) we present the distribution of the $L_{\rm IR}/M_{\rm cl}$ values of CGs (unshaded histograms) and those of opacity class 6 clouds (shaded histograms). The average value of $L_{\rm IR}/M_{\rm cl}$ for 45 CGs is 1.35 $L_\odot/M_\odot$. The average value of $L_{\rm IR}/M_{\rm cl}$ for 29 opacity class 6 clouds, 0.30 $L_\odot/M_\odot$, is found to be significantly lower. In terms of the total stellar mass, the star

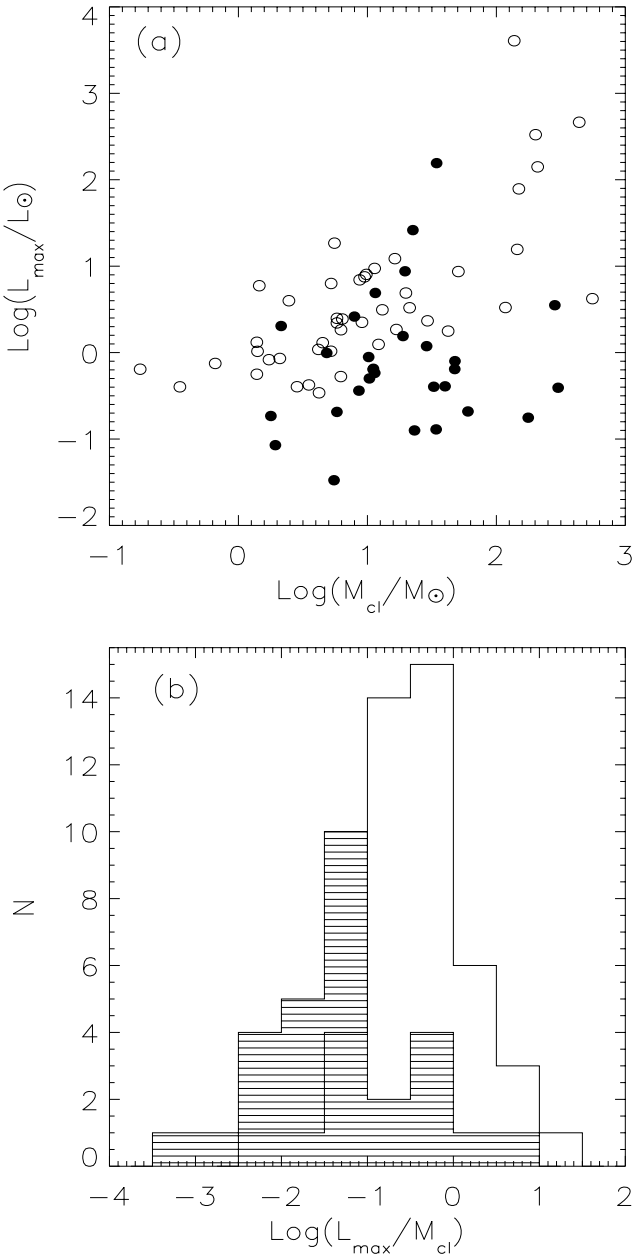

Fig. 4 (**a**) IRAS point-source luminosity vs. parent cloud mass. *Open circles* and *closed circles* denote IRAS sources associated with CGs and opacity class 6 clouds respectively (Parker 1988). (**b**) Distribution of IRAS luminosity to parent cloud mass ratios of CGs (*unshaded histograms*) and opacity class 6 clouds (*shaded histograms*)

formation in CGs is likely to produce more massive stars than that in the opacity class 6 clouds by a factor of ∼2 on the assumption that the IRAS luminosity is related to the stellar mass through $(L/\mathrm{L}_{\odot}) = (M/\mathrm{M}_{\odot})^{3.45}$, the relation for main sequence solar-mass stars (Allen 1973). However, because of the assumption of constant extinction value (5 magnitude) for a number of CGs and the estimation of angular area of CGs from the width of the head, the masses of CGs are to be considered uncertain by a factor of a few. Nevertheless, since the differences are very large, about more than an order of magnitude, we consider that the luminosity-to-mass ratios are systematically larger in the CGs.

The effects of external environments on the luminosities of IRAS sources embedded in bright rimmed clouds and the comparison of their properties with those of BGs were made by Sugitani et al. (1989, 1991). They suggested that stars formed in the HII regions are about 3 times more massive than those in isolated clouds. Dobashi et al. (1996) used data from their large-scale survey of the Cygnus region in ^{13}CO molecular emission line to study the characteristics of molecular clouds and the IRAS sources associated with them (Dobashi et al. 1994). The study was carried out by dividing the clouds into those which are associated with and those which are not associated with the *H II* regions. The Lynds clouds towards the region studied by Dobashi et al. (1996) do show properties similar to the opacity class 6 clouds considered in the present study. For instance, a number of clouds show extinction $\gtrsim$5 mag (Dobashi et al. 2005). From their study, they suggested that the star formation in the *H II* regions is likely to produce more massive stars than in the isolated clouds by a factor of 2–4. Thus, the RDI process believed to as responsible for the star formation in CGs and clouds associated with *H II* region could be producing more massive stars probably by increasing the accretion rates during protostellar stage (Motoyama et al. 2007).

4 Conclusions

We carried out an optical and infrared study of young stellar objects associated with CGs and a comparison with those associated with small, isolated dark globules which are located away from any large star forming regions. Spectroscopy of stars, with nebulosity and/or with Hα in emission, associated with nine star forming CGs are made. The masses of the most massive stars currently associated with CGs are correlated with the mass of the parent cloud but they are systematically larger than expected for clouds of similar mass from the relation in Larson (1982). We also estimated the luminosities of the IRAS sources found associated with CGs as a function of cloud mass and then compared them with those of the IRAS sources found associated with the isolated opacity class 6 clouds (isolated and relatively away from large star forming regions). We found that the luminosities of IRAS sources associated with CGs are larger than those for the opacity class 6 clouds. The average values of the distance independent $L_{\mathrm{IR}}/M_{\mathrm{cl}}$ for 45 CGs and 29 opacity class 6 clouds are ∼1.35 $\mathrm{L}_{\odot}/\mathrm{M}_{\odot}$ and ∼0.30 $\mathrm{L}_{\odot}/\mathrm{M}_{\odot}$ respectively. In terms of the total stellar mass, the star formation in CGs is likely to produce more massive stars than that in the opacity class 6 clouds by a factor of ∼2. These results imply that the massive stars influence star formation

process in clouds like CGs located in their vicinity. The results also supports suggestions from recent simulations that RDI mechanism can increase the accretion rates of protostars near *HII* regions and hence increase the luminosity by 1–2 orders of magnitude compared to those without external triggering.

Acknowledgements We would like to thank the referee for his constructive and helpful comments. The optical images in Fig. 1 are reproduced from the Digital Sky Survey (DSS) which is based on photographic data obtained using the UK Schmidt Telescope operated by the Royal Observatory Edinburgh, with funding from the UK Science and Engineering Research Council and the Anglo-Australian Observatory. The DSS was produced at the Space Telescope Science Institute under the US Government grant NAG W-2166. This publication makes use of data products from the Two Micron All Sky Survey, which is a joint project of the University of Massachusetts and the Infrared Processing and Analysis Center, California Institute of Technology, funded by the National Aeronautics and Space Administration and the National Science Foundation.

References

Alcala, J.M., Wachter, S., Covino, E.: Astron. Astrophys. **416**, 677 (2004)
Allen: 1973, Allen's Astrophysical Quantities, p. 489
Aveni, A.F., Hunter, J.H.: Astron. J. **74**, 1021 (1969)
Bachiller, R., Fuente, A., Kumar, M.S.N.: Astron. Astrophys. **381**, 168 (2002)
Bally, J.: In: Woodward, C.E., Bicay, M.D., Shull, J.M. (eds.) Tetons 4: Galactic Structure, Stars and the Interstellar Medium. ASP Conference Series, vol. 231, p. 204. Astronomical Society of the Pacific, San Francisco (2001). ISBN: 1-58381-064-1
Bertoldi, F.: Astrophys. J. **346**, 735 (1989)
Bertoldi, McKee: Astrophys. J. **354**, 529 (1990)
Bhatt, H.C.: Mon. Not. R. Astron. Soc. **262**, 812 (1993)
Block, D.L., Dyson, J.E., Madsen, C.: Astrophys. J. **390L**, 13 (1992)
Bourke, T.L., Hyland, A.R., Robinson, G.: Mon. Not. R. Astron. Soc. **276**, 1052 (1995)
Brand, P.W.J.L., Harwarden, T.G., Longmore, A.J., et al.: Mon. Not. R. Astron. Soc. **203**, 215 (1983)
Campbell, B., Persson, S.E., Matthews, K.: Astron. J. **98**, 643 (1989)
Cernicharo, J.: The Physics of Star Formation and Early Stellar Evolution. NATO Advanced Science Institute (1991)
Clemens, D.P., Barvainis, R.: Astrophys. J. Suppl. Ser. **68**, 257 (1988)
Clemens, D.P., Yun, J.L., Heyer, M.H.: Astrophys. J. Suppl. Ser. **75**, 877 (1991)
Cohen, M., Kuhi, L.V.: Astrophys. J. Suppl. Ser. **41**, 743 (1979)
Cox, A.N.: In: Cox, A.N. (ed.) Allen's Astrophysical Quantities, 4th edn. AIP/Springer, New York (2000). ISBN: 0387987460
Dickman, R.L.: Astrophys. J. **202**, 50 (1975)
Dobashi, K., Bernard, J.-P., Yonekura, Y., Fukui, Y.: Astrophys. J. Suppl. Ser. **95**, 419 (1994)
Dobashi, K., Bernard, J.-P., Fukui, Y.: Astrophys. J. **466**, 282 (1996)
Dobashi, K., Yonekura, Y., Matsumoto, T.: Publ. Astron. Soc. Jpn. **53**, 85 (2001)
Dobashi, K., Uehara, H., Kandori, R., Sakurai, T., Kaiden, M., Umemoto, T., Sato, F.: Publ. Astron. Soc. Jpn. **57**, 1 (2005)
González-Alfonso, E., Cernicharo, J., Radford, S.J.E.: Astron. Astrophys. **293**, 493 (1995)
Gorti, U., Bhatt, H.C.: Astron. Astrophys. **270**, 426 (1993)
Gyulbudagyan, A.L.: Astrophysics (translated Astrofizika) **23**(2), 533 (1986)
Harju, J., Sahu, M., Henkel, C., Wilson, T.L., et al.: Astron. Astrophys. **233**, 197 (1990)
Hawarden, T.G., Brand, P.W.J.L.: Mon. Not. R. Astron. Soc. **175**, 19 (1976)
Herbig, G.H., Rao, K.N.: Astrophys. J. **174**, 401 (1972)
Herbig, G.H., Bell, K.R.: Lick Observatory Bulletin. Lick Observatory, Santa Cruz (1988)
Herbst, W., Warner, J.W., Miller, D.P., Herzog, A.: Astron. J. **87**, 98 (1982)
Hernádez, J., Calvet, N., Briceño, C., Hartmann, L., Berlind, P.: Astron. J. **127**, 1682 (2004)
Hilton, J., Lahulla, J.F.: Astron. Astrophys. J. Suppl. Ser. **113**, 325 (1995)
Ho, P.T.P., Martin, R.N., Barrett, A.H.: Astrophys. J. **246**, 761 (1981)
Ishii, M., Hirao, T., Nagashima, C., Nagata, T., Sato, S., Yao, Y.: Astron. J. **124**, 430 (2002)
Jacoby, G.H., Hunter, D.A., Christian, C.A.: Astron. Astrophys. J. Suppl. Ser. **56**, 257 (1984)
Jansen, D.J., van Dishoeck, E.F., Black, J.H.: Astron. Astrophys. **282**, 605 (1994)
Jenkins, E.B., Savage, B.D.: Astrophys. J. **187**, 243 (1974)
Kenyon, S.J., Hartmann, L.: Astron. Astrophys. J. Suppl. Ser. **101**, 117 (1995)
Kessel-Deynet, O., Burkert, A.: Mon. Not. R. Astron. Soc. **338**, 545 (2003)
Koornneef, J.: Astron. Astrophys. J. Suppl. Ser. **51**, 489 (1983)
Knude, J., Fabricius, C., Hog, E., Makarov, V.: Astron. Astrophys. **392**, 1069 (2002)
Lada, C.J., Adams, F.C.: Astrophys. J. **393**, 278 (1992)
Larson, R.B.: Mon. Not. R. Astron. Soc. **200**, 159 (1982)
Launhardt, R., Henning, T.: Astron. Astrophys. **326**, 329 (1997)
Lee, C.W., Myers, P.C.: Astron. Astrophys. J. Suppl. Ser. **123**, 233 (1999)
Lefloch, Lazareff: Astron. Astrophys. **289**, 559 (1994)
Lynds, B.T.: Astron. Astrophys. J. Suppl. Ser. **7**, 1 (1962)
Magakian, T.Y.: Astron. Astrophys. **399**, 141 (2003)
Maheswar, G., Manoj, P., Bhatt, H.C.: Mon. Not. R. Astron. Soc. **355**, 1272 (2004)
Maheswar, G., Saurabh, S., Medhi, Biman, J., Pandey, A.K., Bhatt, H.C.: Mon. Not. R. Astron. Soc. **379**, 1237 (2007)
Marco, A., Negueruela, I.: Astron. Astrophys. **406**, 119 (2003)
Miao, J., White, G.J., Nelson, R., Thompson, M., Morgan, L.: Mon. Not. R. Astron. Soc. **369**, 143 (2006)
Motoyama, K., Umemoto, T., Shang, H.: Astron. Astrophys. **467**, 657 (2007)
Myers, P.C., Fuller, G.A., Mathieu, R.D.: Astrophys. J. **319**, 340 (1987)
Myers, P.C., Benson, P.J.: Rev. Mexicana Astron. Astrofis. **7**, 238 (1983)
Nielsen, A.S., Olberg, M., Knude, J., Booth, R.S.: Astron. Astrophys. **336**, 329 (1998)
Odenwald, S.F., Fischer, J., Lockman, F.J., Stemwedel, S.: Astrophys. J. **397**, 174 (1992)
Ogura, K., Hasegawa, T.: Publ. Astron. Soc. Jpn. **35**, 299 (1983)
Ogura, K., Sugitani, K.: Publ. Astron. Soc. Aust. **15**(1), 91–98 (1998)
Olano, Walmsley, Wilson: Astron. Astrophys. **290**, 235 (1994)
Palla, F., Stahler, S.W.: Astrophys. J. **418**, 414 (1993)
Parker, N.D.: Mon. Not. R. Astron. Soc. **235**, 139 (1988)
Pettersson: Astron. Astrophys. **139**, 135 (1984)
Ramesh, B.: Mon. Not. R. Astron. Soc. **276**, 923 (1995)
Reipurth, B.: Astron. Astrophys. **117**, 183 (1983)
Reipurth, B., Gee, G.: Astron. Astrophys. **166**, 148 (1986)
Rieke, G.H., Lebofsky, M.J.: Astrophys. J. **288**, 618 (1985)
Sandqvist: Mon. Not. R. Astron. Soc. **177**, 69 (1976)
Santos, N.C., Yun, J.L., Santos, C.A., Marreiros, R.G.: Astron. J. **116**, 1376 (1998)

Schneps, M.H., Ho, P.T.P., Barret, A.H.: Astrophys. J. **240**, 84 (1980)
Sridharan, T.K.: J. Astrophys. Astron. **13**, 217 (1992)
Strom, S.E., Strom, K.M., Yost, J., Carrasco, L., Grasdalen, G.: Astrophys. J. **173**, 353 (1972)
Sugitani, K., Fukui, Y., Mizuni, A., Ohashi, N.: Astrophys. J. **342L**, 87 (1989)
Sugitani, K., Fukui, Y., Ogura, K.: Astrophys. J. Suppl. Ser. **77**, 59 (1991)
Sugitani, K., Ogura, K.: Astrophys. J. Suppl. Ser. **92**, 163 (1994)
Thé, P.S., de Winter, D., Perez, M.R.: Astrophys. J. Suppl. Ser. **104**, 315 (1994)
Vieira, S.L.A., Corradi, W.J.B., Alencar, S.H.P.: Astron. J. **126**, 2971 (2003)
Vilas-Boas, J.W.S., Myers, P.C., Fuller, G.A.: Astrophys. J. **433**, 96 (1994)
White, G.J.: Astron. Astrophys. **274**, L33 (1993)
Whittet, D.C.B. (ed.): Dust in the Galactic Environment, 2nd edn. Series in Astronomy and Astrophysics. Institute of Physics, Bristol (2003). ISBN 0750306246
Wilking, B.A., Lada, C.J.: Astrophys. J. **274**, 698 (1983)
Williams, P.M., Brand, P.W.J.L., Longmore, A.J., Hawarden, T.G.: Mon. Not. R. Astron. Soc. **181**, 709 (1977)
Zealey, W.J., Ninkov, Z., Rice, E., Hartley, M., Tritton, S.B.: Astrophys. Lett. **23**, 119 (1983)